energies

Article

Performance Analysis Based on Fuel Valve Train Control Optimization of Ammonia-Fuel Ships

Lim Seungtaek, Lee Hosaeng and Seo Youngkyun *

Korea Research Institute of Ships & Ocean Engineering, Daejeon 34103, Republic of Korea; limst@kriso.re.kr (L.S.); hslee@kriso.re.kr (L.H.)
* Correspondence: ykseo@kriso.re.kr; Tel.: +82-055-639-2419

Abstract: In order to reduce carbon emissions, which are currently a problem in the shipping and offshore plant sectors, the international community is strengthening regulations such as the Energy Efficiency Design Index (EEDI) and Energy Efficiency Existing Ship Index (EEXI). To cope with this, eco-friendly fuel propulsion technology is being developed, and the development of an ammonia fuel supply system is in progress. Among them, fuel valve train (FVT) technology was researched for the final supply and cutoff of fuel and purging through nitrogen for ammonia engines. In this paper, we analyzed the change in ammonia supply due to FVT opening and the change in nitrogen supply due to closure. In addition, a plan to minimize risk factors was presented by applying a control method to remove residual fuel in FVT. According to the presented FVT model, the difference in the flow rate of supplied fuel was as much as 17.8 kg/s. Additionally, by opening the gas bleed valve at intervals during the closing process and purging about 0.28 kg of nitrogen, the internal fuel could be completely discharged. This is expected to have an impact on improving the marine environment through the application of eco-friendly fuels and the development of fuel supply system technology.

Keywords: gas valve train; fuel valve train; fuel supply system; ammonia; nitrogen ventilation; main valve; bleed valve

check for updates

Citation: Seungtaek, L.; Hosaeng, L.; Youngkyun, S. Performance Analysis Based on Fuel Valve Train Control Optimization of Ammonia-Fuel Ships. *Energies* **2024**, *17*, 2272. https://doi.org/10.3390/en17102272

Academic Editor: Leszek Chybowski

Received: 12 April 2024
Revised: 30 April 2024
Accepted: 2 May 2024
Published: 8 May 2024

1. Introduction

In response to escalating global concerns regarding maritime pollution, the International Maritime Organization (IMO) is actively discussing measures to enhance operational efficiency through energy policies. This has prompted shipbuilders worldwide to spearhead the development of vessels employing environmentally friendly fuels such as hydrogen, ammonia, and ethanol.

In particular, classification societies have conducted extensive research on various alternative fuels to propose optimal fuels aligned with IMO regulations. Det Norske Veritas·Germanischer Lloyd (DNVGL) (2018) published a guidance paper assessing alternative fuels and technology solutions to facilitate decision-making for ship investments. The paper encompasses an overview of not only selected alternative fuels such as LNG, LPG, methanol, biofuels, and hydrogen but also innovative technologies, including batteries, fuel cell systems, and wind propulsion devices [1].

Lloyd's Register (2020) assessed zero-carbon fuels from an economic perspective and technology perspective. The study proposed 21 zero-emission vessels utilizing fuels such as methanol, hydrogen, ammonia, electricity, diesel, and LNG, alongside production and propulsion methods for natural gas—capable of carbon capture and storage—biomass, and renewable energy [2,3].

Amidst these alternatives, ammonia has emerged as a solution for storage and transportation, finding diverse applications in agriculture, fishery, and refrigeration. MAN B&W aims to develop ammonia-powered vessels by 2024, with the first ship to be an ammonia carrier that facilitates the handling of ammonia [4]. Concurrently, Japanese maritime entities, including NYK Line, Nihon Shipyard, and ClassNK, are actively researching their first utilization of ammonia as a fuel in ammonia transport ships. In addition, NK proposes applicable regulations concerning physical properties of ammonia that require special consideration in terms of flammability and toxicity [5,6].

A report by Smith et al. predicts a 50% reduction in greenhouse gas emissions by 2050 through the adoption of eco-friendly fuels like ammonia and hydrogen in shipping. In addition, DNV analyzed that more than 50% of ship fuel will be converted to LNG, ammonia, etc., by 2050. Figure 1 shows fuel changes by year until 2050 [7,8].

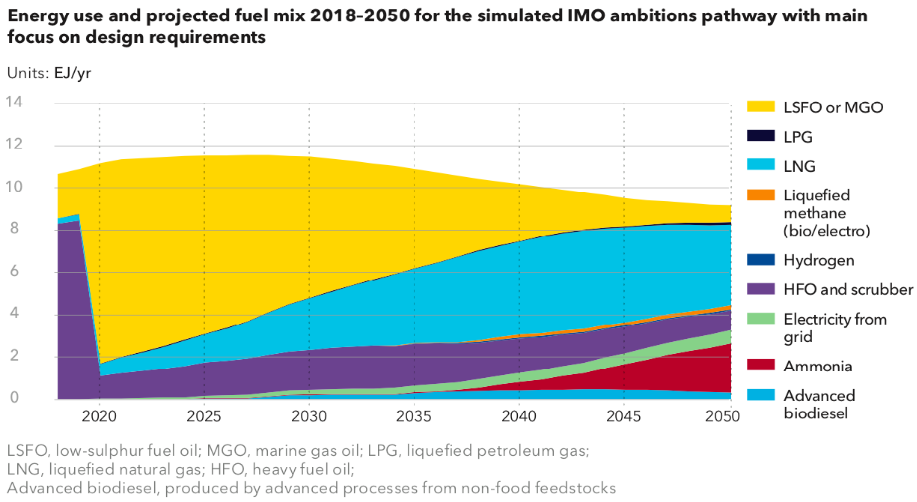

Figure 1. Energy use and projected fuel mix 2018–2050 for the simulated IMO ambitions pathway with main focus on design requirements (Source: DNV).

The International Maritime Organization (IMO) has set ambitious targets for reductions in GHG emissions. Total GHG emissions should fall by at least 50% and CO_2 emissions should fall by at least 70% below the 2008 figures by 2050 [9]. Consequently, DNV suggested that by 2050, at least 15% of long-distance ships should be fueled by ammonia or hydrogen [10].

Ongoing research is dedicated to engine systems utilizing ammonia fuel and related fuel supply systems. Studies on ammonia engines include dual-fuel applications with diesel engines [11,12] and analyses of fuel characteristics in single-fuel configurations [13]. Ammonia application in ships is evolving with a focus on classification [14], while universities and research institutes are conducting research for technology development [15].

In particular, Seo et al. evaluated the economic feasibility of ammonia-fuel carriers based on different fuel storage methods, shedding light on the influence of storage methods on cost variations. Additionally, Julia et al. suggested a high production potential for ammonia fuel, considering its technical, environmental, and economic viability in ship fuel applications [16,17].

As of 2024, over 90% of a vessel's fuel comprises fossil energy-based fuels such as heavy fuel oil (HFO) and marine diesel oil (MDO), with alternative fuels like LNG and biofuels. CO_2 emissions are thus inevitable [18]. To replace such fossil fuels with ammonia, it is essential to consider the heating value of the fuel required to maintain a vessel's propulsion capacity.

Also, ammonia, with its high density and relatively lower heating value, results in approximately 2.2 times higher fuel consumption compared to conventional fuels [19]. This necessitates substantial fuel storage facilities to accommodate the increased fuel consumption. According to the National Fire Protection Association (NFPA)'s hazard index table, ammonia is an extreme danger; level 3 in health hazard, and is a fluid with an ignition point at 200 F. Therefore, it is applied according to usage regulations, and typically in compliance with the regulations of ISO 23306:2020 [20]. These risks and low efficiency are obstacles to the application of ammonia engines despite their high environmental improvement rates.

In order to minimize the risk of ammonia, stabilization research is inevitable through the structure or control of the fuel supply system (FSS) and fuel valve train (FVT). Among them, FVT serves as the pivotal system connecting the fuel supply system and the final connection valve system, providing fuel such as liquefied natural gas (LNG), liquefied petroleum gas (LPG), and ammonia to the engine in maritime vessels [21]. In engines utilizing gaseous fuels like LNG, the system is referred to as the gas valve train; however, for consistency in this paper, we adopt the unified term "FVT" to denote the concept of fuel. The FVT plays a crucial role in controlling the supply and shut-off of fuel, and performing nitrogen-assisted ventilation during the fuel shut-off process, thereby maintaining safe engine operation. Figure 2 illustrates the fuel supply system for a ship utilizing ammonia. Here, fuel is supplied from the high pressure (HP) pump in the FSS to the FVT, and upon valve opening, the fuel is delivered to the final engine. Nitrogen (N_2)-purging facilities are connected to both systems to prevent residual fuel, and pressurized N_2 inside the pipes is exhausted externally [22,23].

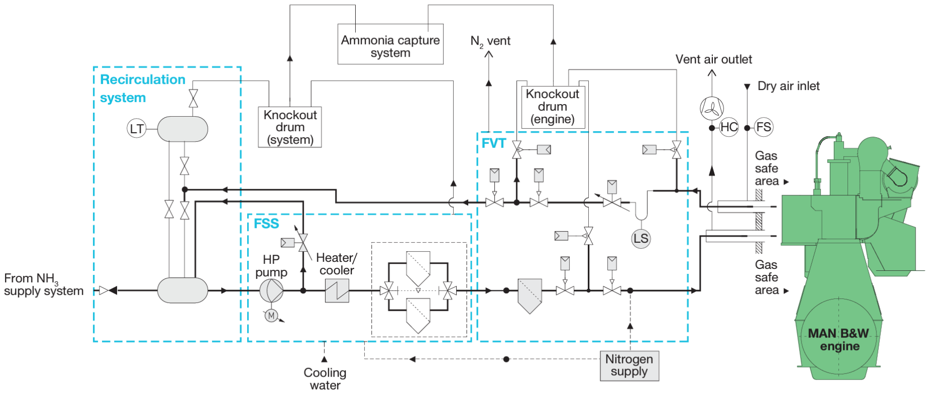

Figure 2. Principles of the ammonia supply system, showing main components (Source: Man B&W).

The primary function of the FVT is to supply and shut off fuel to the engine. Consequently, variations in fuel supply time occur depending on the opening time of the fuel supply valve during fuel supply.

Fuel shut-off requires distinct operating procedures due to differences between regular engine shutdown and emergency shutdown during fire or emergencies. In the case of a regular shutdown, fuel must be completely purged from the engine for long-term engine stoppage and maintenance reasons. Moreover, precautions must be taken to prevent potential hazards such as fuel leakage and fire after shutdown. During this process, fuel purging and internal ventilation are performed through bleed valves, utilizing N_2 gas to remove fuel from fuel supply devices and the engine inlet/outlet.

In contrast, emergency fuel shutdown arises in situations necessitating abrupt engine shutdown or engine damage. In such cases, the rapid closure of the fuel valve is essential. Similar to a regular shutdown, N_2 is employed to ventilate fuel supply devices and the engine inlet/outlet, concluding the final shutdown process swiftly and safely.

In the case of the currently commercialized GVU model of LNG fuel, a fully ex-proof encapsulated design is applied to completely block fuel emission to the outside. However, the area occupied by the external protection device is larger than that of the GVU, and a detection device for exposed fuel is essential. In addition, an increase in initial costs due to these structural changes and additional facilities is inevitable [24].

Holger Watter presented a gas valve unit (GVU) operation model according to load changes in LNG-fueled propulsion ships, and Lee studied fuel switching and gas leakage prevention through GVU stoppage in emergency situations while using gas fuel in a dual-fuel engine [25,26].

However, few studies exist on the operation of the fuel valve train (FVT) using ammonia fuel, responsible for overseeing the final fuel supply to the engine and purging residual fuel within the pipes via N_2. This paper aims to fill this gap by establishing and analyzing the operation of FVT, a key component of emerging ammonia-powered vessels. Conventional and newly applied operation methods are compared to assess the resulting improvements.

2. FVT Analysis Conditions

2.1. Theory

2.1.1. Valve Size and Controller Selection

The coefficient of flow, denoted as C_v, represents the flow characteristics in valves and is commonly referred to as the flow coefficient. It is a numerical value used to calculate flow rates. C_v signifies the flow rate (in gallons per minute, GPM) through a valve under a pressure difference of 1 psi at 60 °F. The selected C_v maintains a pressure difference of less than 10 kPa between the main valve and bleed valve while satisfying the required flow for fuel supply. Equation (1) represents the calculation formula for determining C_v, where Q is the flow rate, SG is the specific gravity of ammonia fuel, and P is the pressure drop [27].

$$C_v = Q\sqrt{\frac{SG}{\Delta P}} \tag{1}$$

The valve mode defines the relationship between the desired actuator position and current actuator position. The desired actuator position can be set by a proportional–integral–differential (PID) controller. A controller's output (OP), for instance, is exported to the desired actuator position. Depending on the valve mode, the current actuator position can behave in one of the following three ways: (1) quick open mode, (2) equal percentage mode, or (3) linear mode [28].

For this simulation, linear mode was selected. The actuator can be modeled to move to the desired actuator position at a constant rate. The actuator moves according to Equation (2). The actuator position is converted sequentially until the final required point (Equation (3)), if the desired actuator position is above the current actuator position. The linear rate can be specified in the actuator linear rate. Typical stroke times (closure rates) are as follows: (1) electric–hydraulic actuators: approximately 12 inches/minute, (2) piston actuators (motor-driven): under 70 inches/minute [29].

$$Act\% = (Actuator\ Linear\ Rate)\Delta t + Act_o\% \tag{2}$$

$$until\ Act\% = Act_{Desired}\% \tag{3}$$

where Act is an abbreviation for Actuator position, t is time, and the subscript Act_o means initial actuator position.

2.1.2. Nitrogen Supply Selection

The nitrogen buffer capacity is the sum of the nitrogen volume required for ammonia-fuel engine operation and the additional nitrogen volume required for the low-flashpoint fuel supply system (LFSS) and other upstream systems that also connect to the nitrogen buffer (Equation (4)) [30].

$$V_{buffer} = V_{buffer}, ME + V_{buffer}, LFSS \tag{4}$$

It is the scope of the shipyard to determine the capacity of any additional nitrogen requirement, V_{buffer} of ME and LFSS. For purging purposes of the main engine with LPG fuel, the minimum required nitrogen volume capacity is calculated according to Equation (5).

$$V_{buffer,}ME = (10 \times P_{purge} \times V_{purge}) \times z/(P_{buffer} - P_{purge}) \tag{5}$$

In Equation (6), P_{purge} is the target pressure for pressurization during liquid freeing, which must be 700 kPa higher than the back pressure from the service tank or the nitrogen separator.

$$P_{purge} = P_{service\ tank} + 700(\text{kPa}) \tag{6}$$

V_{purge} is the total internal volume of piping going from the nitrogen supply line to the engine vent and comprises the following volumes:

- The LFF supply line going from the FVT to the engine;
- The internal LFF volume of the engine;
- The circulation line going from the engine to the vent connection.

Z represents a minimum number of times of purging the engine which should be immediately available. Assuming that on-board nitrogen production is available, engine makers recommend that z should be at least equal to 3 consecutive LFF starts. P_{buffer} is the storage pressure of the nitrogen, of which only the pressure exceeding P_{purge} is available for the purging of the engine. $P_{service\ tank}$ is the pressure of the service tank.

2.2. System Design

2.2.1. Fuel Supply Module Design

To analyze the ammonia fuel consumption of ammonia-powered ships, a fuel supply system was designed. Ammonia fuel is stored in a service tank and supplied during vessel operation, with fuel injection conditions for engine supply controlled at a temperature of 35 °C or higher and a pressure of 8000 kPa through the fuel treatment system. The structure of the fuel supply system and FVT used Man B&W's ammonia supply system [4]. The performance table for each eco-friendly fuel is shown in Table 1.

Table 1. Comparison table for each eco-friendly fuel.

	Energy Content, LHV [MJ/kg]	Energy Density [MJ/L]	Supply Pressure [kPa]	CO_2 Reduction Compared to HFO Tier II [%]
Ammonia (NH_3)	18.6	10.6	8000	90
Methanol (CH_3OH)	19.9	14.9	8000	11
LPG	46.0	26.7	1000	13–18
LNG	50.0	21.2	5000	24
MGO	42.7	35.7	30,000	0
Hydrogen (H_2)	120	8.5		

During this process, fuel distribution to the engine and the circulation of return fuel are controlled through the FVT. The vaporization and heating of liquid ammonia are achieved through heat exchange with steam or seawater using the glycol water system. In FVT, the two main valves are doubled for safety, and the engine is purged with nitrogen to remove internal ammonia.

The formula for calculating fuel consumption is provided in Equation (7). Vessel fuel consumption varies based on the type of fuel, engine size, and endurance, with different ammonia carriers having different consumption rates. Figure 3 illustrates the changes in ammonia fuel supply and return rate. Here, the fuel supply rate refers to the amount of fuel flowing into the engine per hour, and the recirculation percentage is the fuel return rate that remains and circulates without being supplied to the engine.

The fuel supply rate was calculated using the heating value of ammonia to achieve a capacity of 16,080 kW, enabling a supply of 5909 kg/h at maximum 100% load conditions. At this time, 5.5% of fuel circulates to the pump and tank. In the initial low-load condition of less than 10, about 115 kg/h of fuel is supplied to the engine and 82.7%, or 551 kg/h, is circulated. On the other hand, the amount of fuel circulated was the highest under the condition of 50% engine load, and this result is expected to indicate that the amount circulated is high compared to the amount flowing into the engine in the total fuel supply amount. Where LHV means lower heating value, and HFO means heavy fuel oil.

$$\text{Fuel consumption of Ammonia} = \text{Fuel consumtion of HFO}\frac{\text{LHV of HFO}}{\text{LHV of Ammonia}} \quad (7)$$

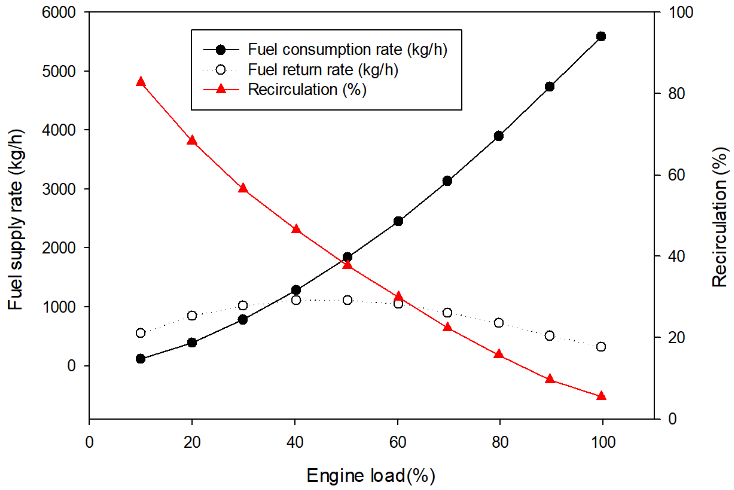

Figure 3. Fuel supply rate and recirculation according to engine load.

To analyze the fuel supply system and fuel valve train, the process design software AspenTech HYSYS (V12.1) was employed as the simulation and analysis tool. HYSYS has the advantage of accurately calculating state values necessary for thermodynamic cycle simulation, making it suitable for this study [31]. The thermodynamic and transport properties of the working fluid are used in conjunction based on the REFPROP database. Ammonia and nitrogen are used as the engine fuel and purging gas. The initial conditions are listed in Table 2 [32,33].

The ideal part of the fundamental equation is given by Equation (8).

$$\frac{a(\rho,\ T)}{RT} = \alpha(\delta,\ \tau) = \alpha^0(\delta,\ \tau) + \alpha^r(\delta,\ \tau) \quad (8)$$

where a is the Helmholtz energy, $\delta = p/p_c$, $\tau = T_c/T$, the superscript 0 refers to the ideal gas Helmholtz energy, and the superscript r refers to the residual Helmholtz energy. The subscript c refers to the critical value. p stands for pressure and T stands for temperature.

The ideal gas Helmholtz energy equation can then be expressed as Equation (9).

$$\alpha^0 = \ln\delta + 2.500571\ln\tau - 12.76941 - 0.00813787\tau - 1.0150785\times10^{-7}\tau^{-7} \quad (9)$$

The residual Helmholtz energy contribution to the equation of state is given by Equation (10). Where M, I, and j are constants.

$$\alpha^r(\delta,\ \tau) = \sum_{k=1}^{10} M_k\delta^{i_k}\tau^{j_k} \quad (10)$$

2.2.2. FVT Design

The FVT receives ammonia fuel from the fuel supply system, distributes it to each cylinder, and recirculates some residual fuel to the fuel recirculating system. Liquid ammonia is supplied back to the inlet of the two-stage fuel pump in the fuel supply system.

The fuel flow is regulated based on engine load variations through the cylinder supply control valve. The ratio of recirculated fuel and the amount of fuel supplied by the fuel pump varies with engine load. Figure 4 illustrates the piping process delivering fuel to the six-cylinder engine through the FVT.

When converting a diesel-fueled vessel to ammonia, for a 6-cylinder engine, a maximum fuel consumption of 5909 kg/h (984.8 kg/h per cylinder) is required at full load. However, the recirculation is approximately 5.47%, resulting in 341 kg/h of fuel being returned by the FVT. The recirculation increases up to a maximum of 83% with load variations. Additionally, nitrogen gas is supplied to the main gas valve inlet and outlet of the

FVT, and the internal ammonia is vented into the atmosphere. The main gas valve and gas bleed valve operate according to the operation logic appropriate for each situation.

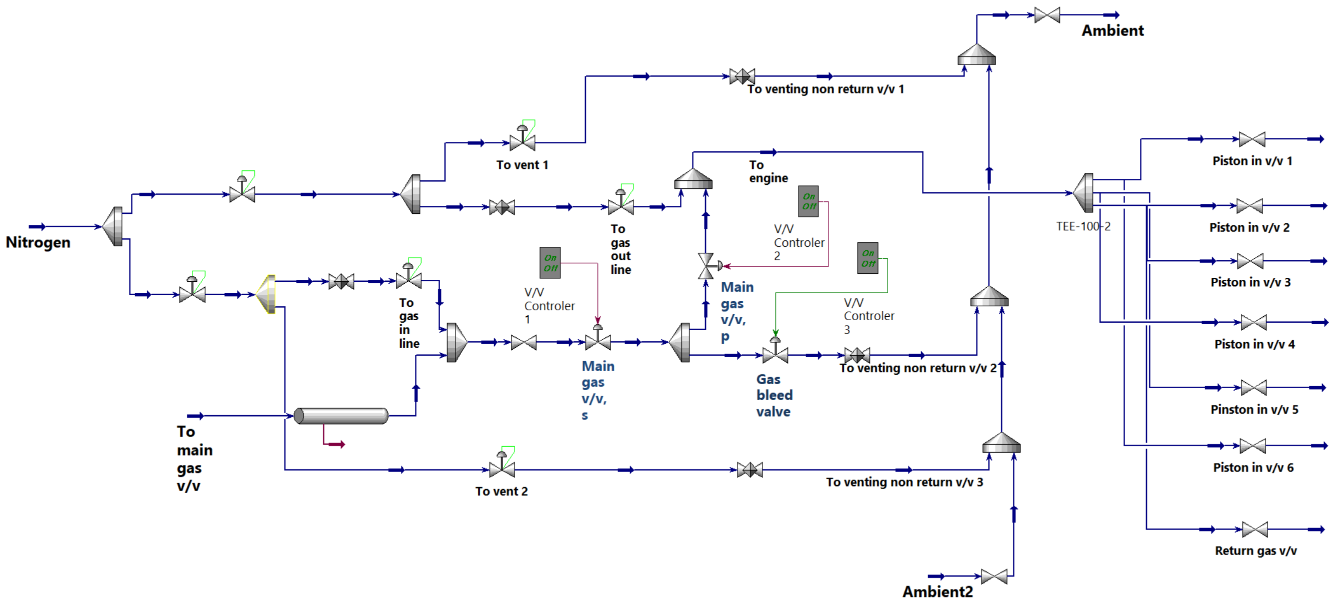

Figure 4. Piping process delivering fuel to the six-cylinder engine through the FVT.

At this time, ammonia was supplied through a high-pressure pump and heater, and a pressure of over 8000 kPa and a temperature of 35 °C were applied [4]. Additionally, in the case of nitrogen, a purging pressure of 30 °C and 800 kPa, similar to atmospheric temperature, was applied [30].

In this paper, FVT was designed during the start and stop process of an ammonia engine and its performance characteristics were analyzed. However, purging characteristics according to the structure of the ship and piping were not considered, and the performance characteristics according to the purging capacity commonly applied by engine companies were analyzed through simulation.

Table 2. Operating conditions of fuel and purging gas of FVT.

	Simulation Data	Reference
Fuel Condition		
Fuel Inlet Temperature [°C]	35	[4]
Fuel Inlet Pressure [kPa]	8000	[4,30]
Mass Density [kg/m^3]	594.58	[31]
Mass Heat Capacity [kJ/kg-°C]	4.78	[31]
Thermal Conductivity [W/m-°C]	0.462	[31]
Viscosity [cP]	0.121	[31]
Purging gas condition		
Purging Gas Inlet Temperature [°C]	30	
Purging Gas Inlet Pressure [kPa]	800	[26,34]
Mass Density [kg/m^3]	8.90	[32]
Mass Heat Capacity [kJ/kg-°C]	1.05	[32]
Thermal Conductivity [W/m-°C]	0.026	[32]
Viscosity [cP]	0.018	[32]

2.2.3. Selection of Valve Size and Nitrogen Supply

The valves controlled by the FVT include one master valve, two main valves, and an intermediate bleed valve for ammonia discharge. The valve sizes are selected with a C_v

value of 50 to minimize pressure drop at the maximum flow rate, thereby minimizing valve size and lowering the budget. The pressure change with respect to C_v variation is depicted in Figure 5a. The selected C_v value ensures that the pressure drop, measured as 2.9 kPa, for ammonia fuel passing through the main valve does not exceed 3 kPa.

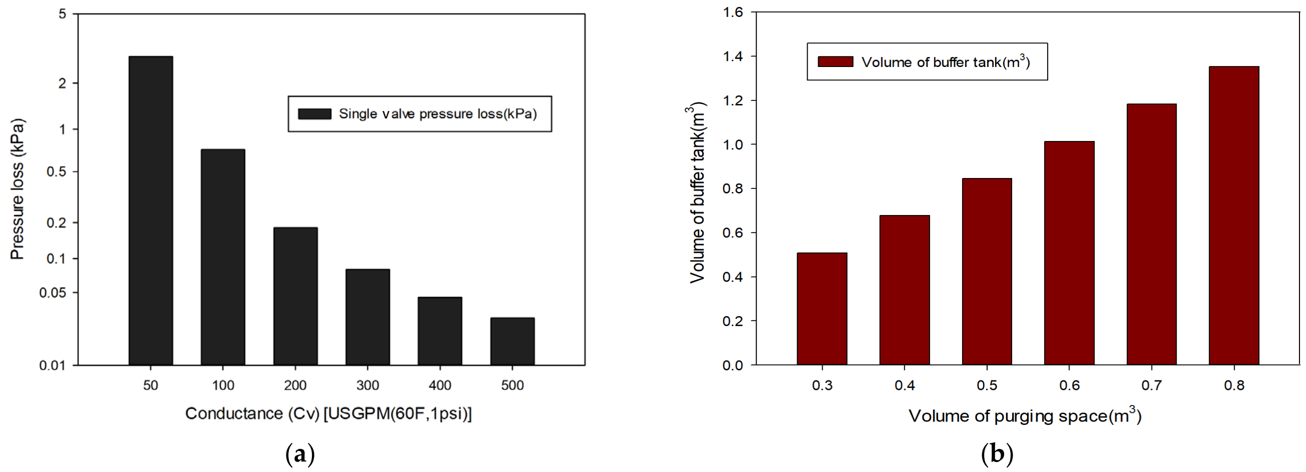

Figure 5. (**a**) Pressure change according to C_v change; (**b**) volume of buffer tank in relation to volume of purging space.

To analyze the nitrogen supply, the total nitrogen storage capacity was estimated for a 15,000 kPa high-pressure storage tank, assuming that pipe areas from the fuel supply system (FSS) to the nitrogen discharge valve at the engine ranges from 0.3 to 0.8 m^3.

Figure 5b illustrates the buffer tank's capacity based on the purging space. Assuming that the purging space is 0.5 m^3, approximately 0.845 m^3 is required for ammonia storage. These results will be compared with the nitrogen capacity consumed in simulation models.

Additionally, according to the purging design for ship engines worldwide, nitrogen pressure operates between approximately 800 kPa and a maximum of 1500 kPa [33–35]. In the FVT-based ship fuel supply system, variations in pressure lead to differences in the rate and time of residual ammonia discharge from the engine. Table 3 presents the purging pressure variations for current dual-fuel engines or gas-fuel engines in ships.

Table 3. Purging pressure of a dual-fuel engine or gas-fuel engine.

Engine Producer	Wärtsilä [33]	MAN B&W [26]	HiMSEN Diesel Engine [34]	Win GD [35]
Name of model	16V50DF	G60ME-C9.2-GI-TII	H54DFV	X92DF
Engine capacity [kW]	15,600	21,440	25,200	63,840
Reference pressure [kPa]	1500	700~900	850~1050	1000~1500

3. Analysis of Control Application Characteristics

3.1. FVT Startup during Engine Operation

3.1.1. Logic for Startup

The startup of the ammonia engine occurs when the final engine supply valve opens, securing fuel supply from the moment the initial fuel supply pump and the ammonia heating system are active. As the load increases, the fuel supply valves of each cylinder progressively open, leading to an increase in the fuel supply rate. Figure 6 illustrates the simplified startup logic of the ammonia engine.

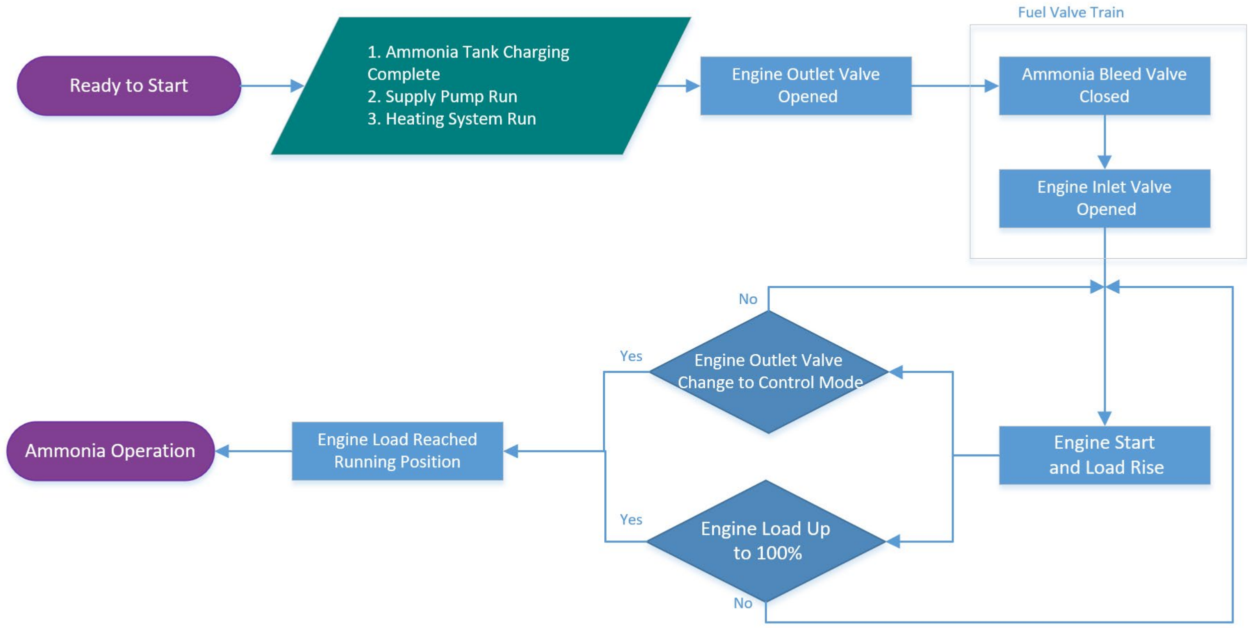

Figure 6. Simplified startup logic of ammonia engine.

During the operational procedure, the FVT starts when the bleed valve closes, simultaneously with the opening of the two main valves, supplying fuel to the engine. Each valve operates based on the actuator's opening time, and in the case of conventional LPG vessels, each valve has a maximum operating range of 10 s. However, during the startup process, the bleed valve closes, and the main valves open. Afterwards, the engine is operated manually and the maximum load is reached by raising the telegraph by the operator. At this time, the system is converted to normal running mode only when the final load condition is reached and the engine outlet valve is completely converted to control mode.

The operation begins only after completely venting the internal N_2 and securing liquid ammonia. Therefore, there are no risks related to opening time. However, the time to reach the appropriate flow rate and nitrogen composition are factors that delay the time until engine start. In addition, to verify the fuel transition within the pipes, engine performance was compared in consideration of the actuator's opening time.

In this study, the actuator's operating range was determined to be 2–10 s [30]. Comparative analysis was performed for the flow rate and ammonia and nitrogen composition of the fuel supplied to the engine in relation to the opening and closing of the bleed and main valves. Through dynamic simulation, the FVT opening rate with rapid increase in flow rate and rapid change in ammonia composition was derived.

3.1.2. Control Application Characteristics for Startup

During the engine startup, the main gas valve opens, and nitrogen in the pipes is bypassed to the knockout drum and circulated until all N_2 is completely removed. This leaves only the liquid ammonia to circulate. To achieve maximum ammonia supply in a short time while ensuring the complete removal of FVT's N_2 gas, the opening time of the main valve was analyzed. Regardless of the main valve's opening time, approximately 131.9 s were required to reach the maximum flow of 746 kg/h. On the other hand, the time to reach 50% of the maximum flow was 20.3 s after the main valves were opened, and depending on the valve opening rate, a flow difference of 4.78% (17.8 kg/h) occurred at a 30%/s opening rate. However, at the 80% point of the maximum flow at 47.4 s after the main valves were opened, the difference due to the valve opening rate showed only a minor increase of 0.56% (3.4 kg/h), indicating a diminishing impact of the valve opening rate on flow increase. The fuel flow rate and ammonia composition for the FVT's main valve with a 10% opening rate are depicted in Figure 7. Furthermore, the ammonia conversion rate based on valve control conditions showed that the ammonia conversion reached 98.0% in the engine return pipe 67.8 s after the main valves were opened. After 200 s, the ammonia conversion rate reached 999,926.1 ppm (99.99%). On the other hand, residual nitrogen is expected to cause NOX generation during the combustion process along with air. Therefore, it is expected that engine startup will be necessary after the ammonia composition inside the system has been converted to 99.99% [36].

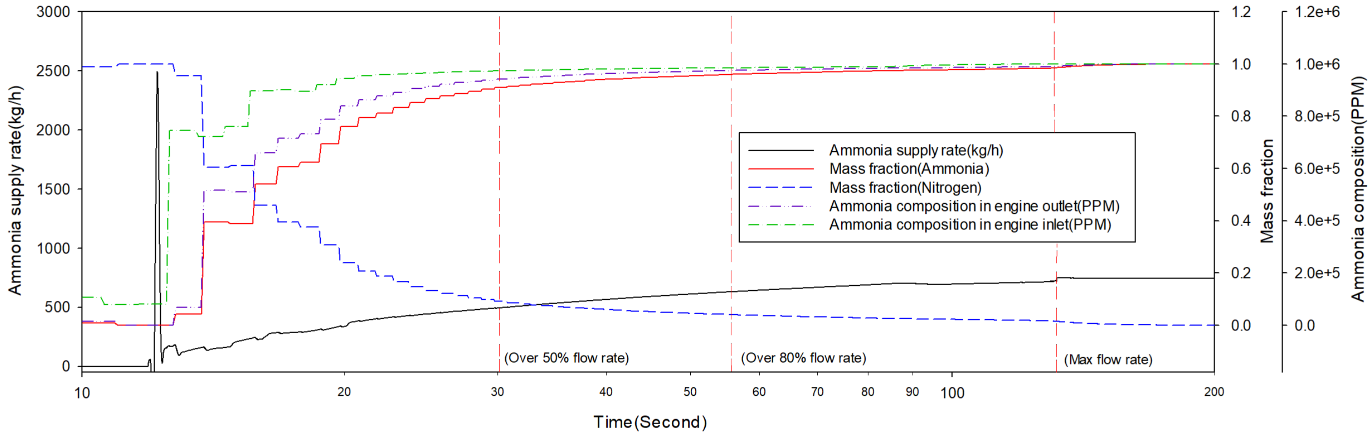

Figure 7. Fuel flow rate and ammonia composition due to the opening of the main valve of FVT with a 10% opening rate.

Figure 8a,b show the changes in fuel supply and ammonia composition in relation to valve opening rate. Under the condition of an opening rate of 20%/s, in Figure 8a,b, an increase in flow rate of 3.4 kg/h compared to the previous one was confirmed and the difference in ammonia conversion up to 98% in relation to valve opening rates was negligible, with less than 0.03% (245 ppm) variation.

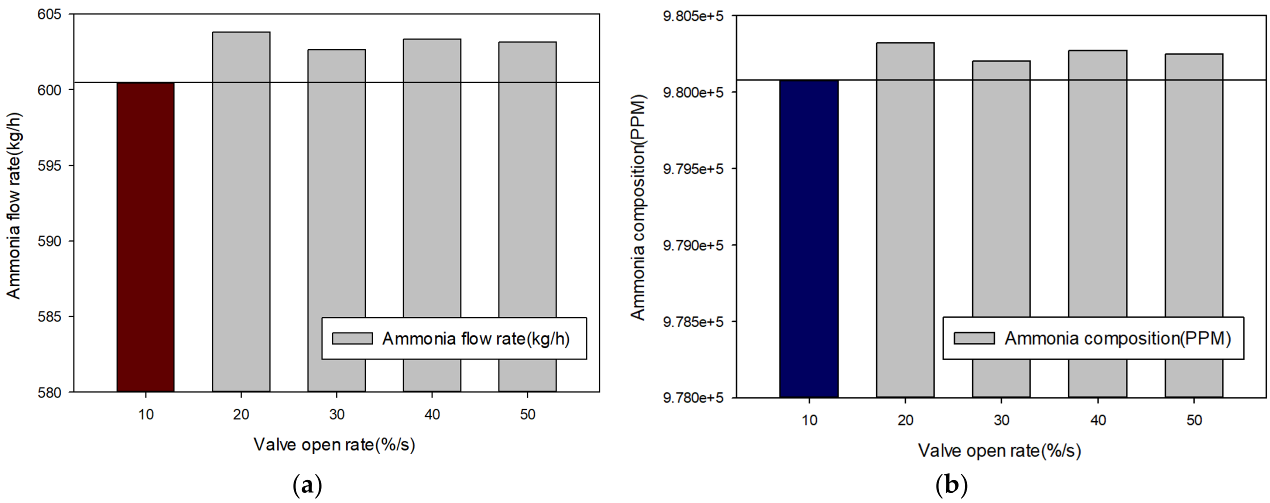

Figure 8. (**a**) Ammonia supply rate change in relation to valve opening rate; (**b**) ammonia composition change in relation to valve opening rate.

In the study proposed through experiments by Chun et al., by opening the GVU after starting the LNG fuel propulsion engine, a high flow rate increase of about 9 times the initial flow rate (20.5 times for this model) occurs. This phenomenon is expected to increase the flow rate due to changes in flow rate as high-pressure liquid ammonia flows into the pipe filled with low-pressure nitrogen gas after ventilation. In addition, the initial increase rate of flow rate is expected to vary depending on the supply pressure of 600 kPa and 8000 kPa for LNG and ammonia. Afterwards, it was designed to gradually increase the flow rate with increasing load under low-load conditions [37]. Through comparison with this actual model, the operating accuracy of the proposed ammonia analysis model can be confirmed.

3.2. FVT Startup during Engine Shutdown

3.2.1. Logic for Shutdown

The ship's stopping methods include routine stops at ports or designated locations and emergency stops in urgent situations such as fire or collision. In a typical operational stop, the supply of fuel to the engine is cut off by closing the main valve, and any remaining ammonia fuel within the pipes is discharged through the bleed valve and the purging valve at the engine outlet via N_2 purging. This approach makes repair and maintenance more convenient and prevents potential fires due to pipe leaks.

In contrast, emergency stops prioritize the safety of the vessel and crew over engine maintenance. Risks are minimized by swiftly cutting off the fuel and purging any remaining fuel. Accordingly, it is essential to follow the existing shutdown logic, rapidly closing the main gas valve within two seconds and subsequently purging the residual fuel supplied to the engine via N_2 purging.

Figure 9a illustrates the conventional FVT operating logic during the shutdown process, without considering ordinary or emergency situations. In this scenario, the main valve is controlled with a two-second limit on the actuator, while the gas bleed valve is limited to a 10 s opening time. Afterwards, the fuel valve on the engine outlet side is blocked, and the bypass valve of the FVT is opened. Consequently, there is a segment where purging between the main gas valve and gas bleed valve fails, and residual ammonia may be present during maintenance or management.

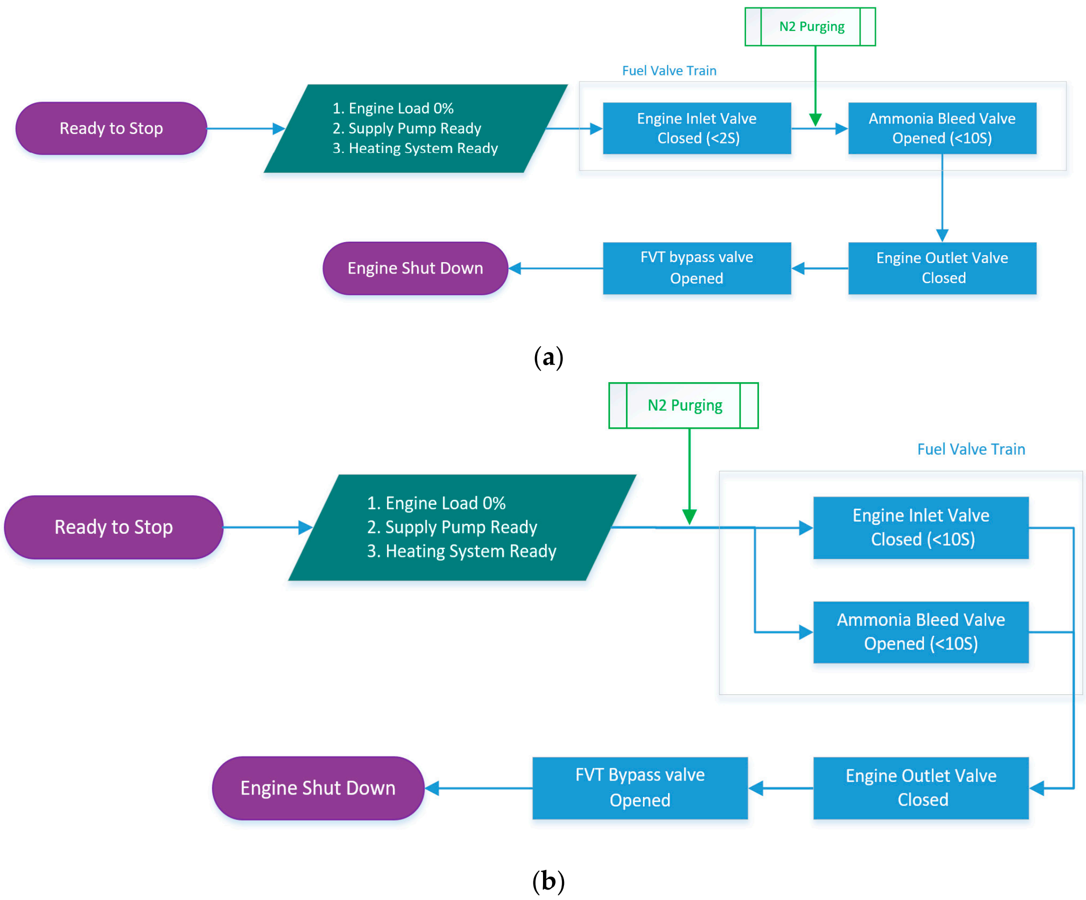

Figure 9. (**a**) FVT operating logic during engine shutdown of a ship; (**b**) newly proposed FVT operating logic.

Hence, in this simulation, for general shutdown processes in non-emergency conditions, the main valve is set up to completely purge ammonia through the bleed valve during the 2 to 10 s closing process. Figure 9b presents the N_2 purging logic behind the simulation [30]. At this time, the stop logic is constructed based on the state in which more than 99.995% of ammonia has been removed, and exposures to levels exceeding 50 ppm result in immediate irritation to the nose and throat. [38]

This operation method can be used to check operation performance by constructing valve opening and closing diagrams through the development of the actual FVT control model presented by Kang et al. [22].

3.2.2. Control Application Characteristics for Shutdown

In the conventional engine shutdown process, the main valve is locked, followed by the removal of ammonia from the pump side and engine inlet using nitrogen. After one second, the bleed valve opens. Figure 10 depicts the distribution of ammonia and the change in N_2 during the engine shutdown process. With an N_2 supply of 5148 kg/h, the ammonia distribution decreases to below 1 ppm after 294 s for the pump side and 305.5 s for the engine side. However, the ammonia concentration exceeds 600,000 ppm until about 278 s, and then tends to decrease rapidly. In this phenomenon, the liquid ammonia remaining inside the pipe is naturally vaporized, maintaining the ammonia composition, but it is expected to decrease rapidly after it is completely vaporized. Moreover, the numerical value of ammonia discharged through the bleed valve is 1,000,000 ppm (100% ammonia), confirming the presence of residual liquid ammonia within the FVT.

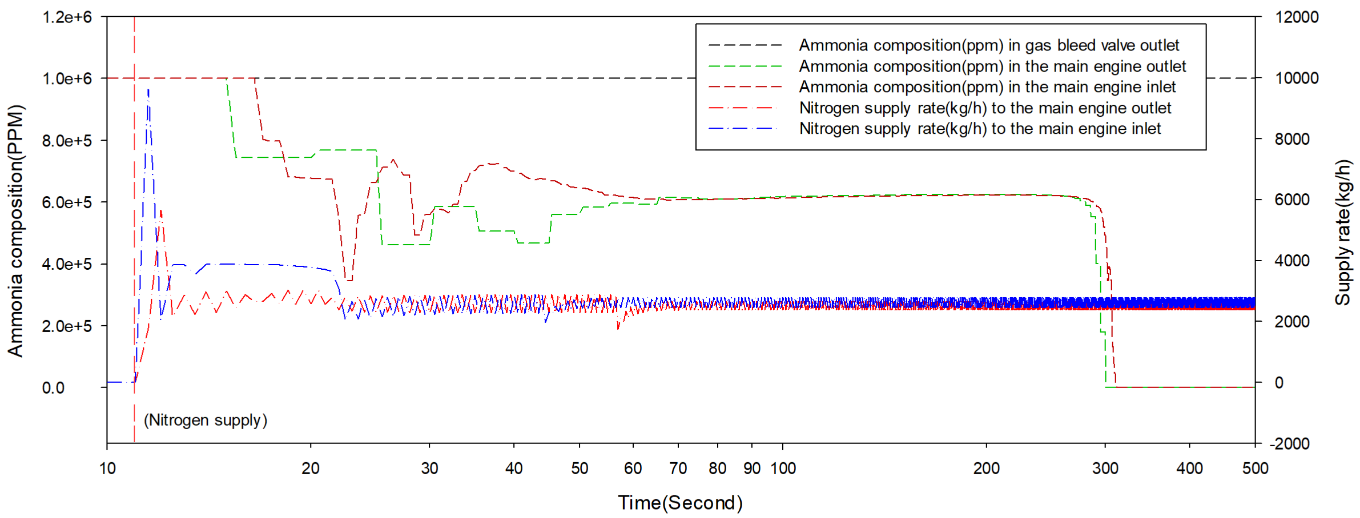

Figure 10. Ammonia composition and N_2 supply rate changes during engine shutdown.

Additionally, the analysis examined an increase in the purging pressure from 800 kPa to 1600 kPa. The time required for N_2 consumption and ammonia distribution to decrease below 1 ppm was investigated. Figure 11a,b illustrate the supply of N_2 entering each pump and engine, and the purging time. When supplying nitrogen at 1600 kPa, the engine and pump had minimum times of 149 s and 205.5 s, respectively. The N_2 consumption, relative to the supply flow over time, amounted to 1.25 m^3 at 1200 kPa pressure for the engine and 1.42 m^3 at 800 kPa for the pump.

The amount of N_2 required to purge the 0.5 m^3 space provided by the engine manufacturer is 0.845 m^3. However, this simulation required an additional supply of about 48.1% of N_2 from the pump side and about 81.3% of N_2 from the engine side to achieve an ammonia removal rate of over 99.995%.

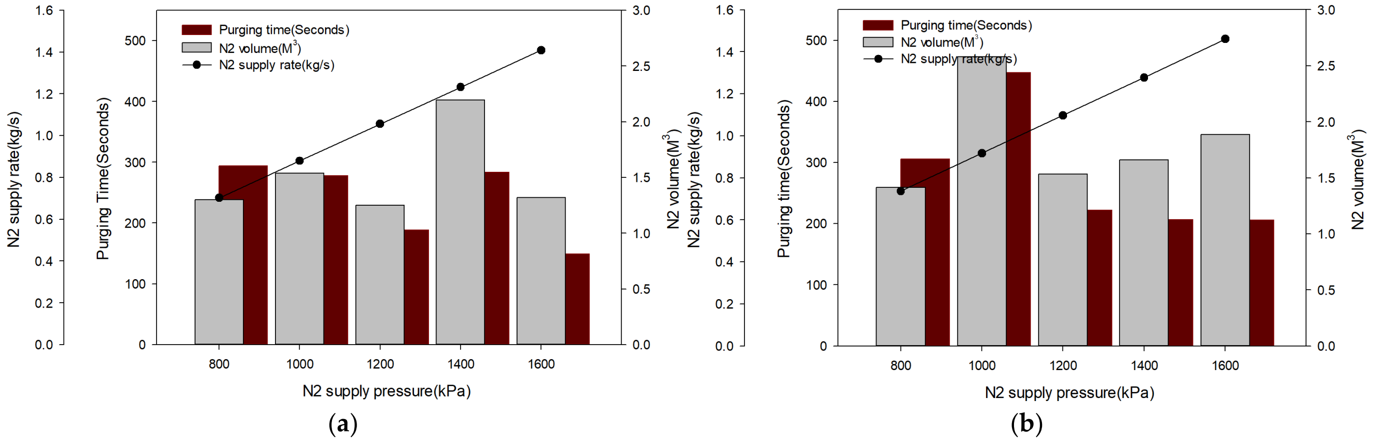

Figure 11. (**a**) N_2 flow rate and pump and purging time of the pump side; (**b**) N_2 flow rate and pump and purging time of the engine outlet side.

This study also compared the amount of nitrogen discharged and the time required for complete ammonia removal when applying valve opening variations that prevent residual ammonia in the FVT. Initially, changes in the opening of the main valve showed that complete ammonia removal occurred only at rates of 10–20%/s. If the fuel valve is shut off within five seconds, some ammonia remains in the FVT. A range of 10–30%/s was considered for the operation of the bleed valve with valve opening. Control times were selected at 10%/s for the gas bleed valve and 18%/s for the main gas valve to minimize nitrogen discharge through the bleed valve. In this case, the amount of N_2 supplied until complete ammonia removal was 0.28 kg. Maximum nitrogen consumption was achieved when the opening was 30%/s for the gas bleed valve and 10%/s for the main gas valve. The N_2 supply was 1.01 kg, representing a 360% increase compared to the minimum supply amount. Figure 12a illustrates the nitrogen consumption based on variations in the gas bleed valve and main gas valve opening.

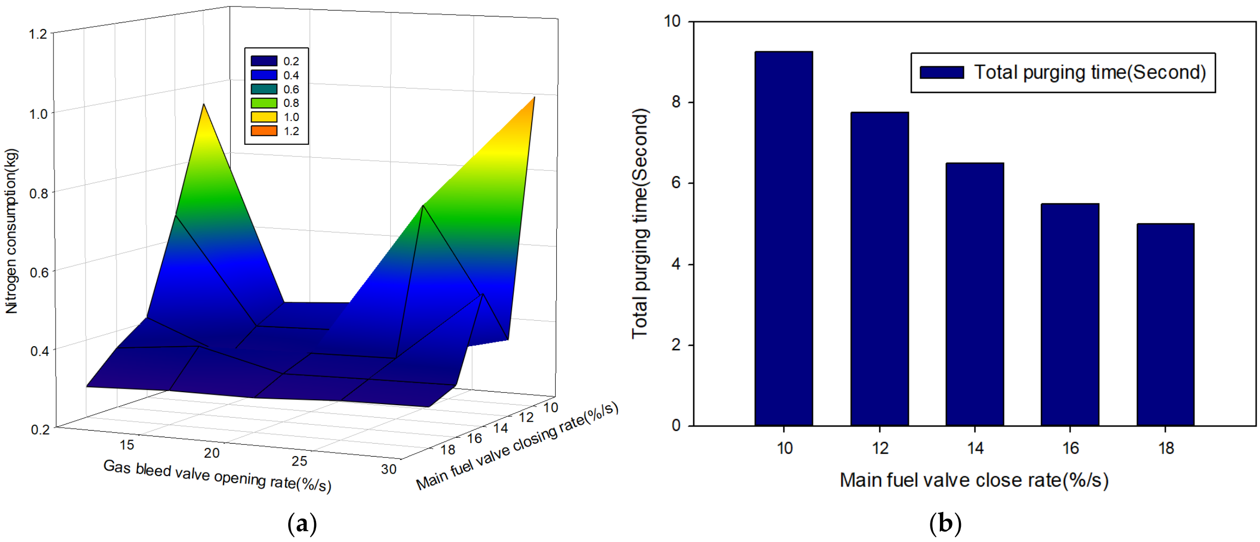

Figure 12. (**a**) Nitrogen consumption in relation to opening rates of gas bleed valve and to closing rates of main gas valve; (**b**) changes in purging time in relation to main gas valve closing rate.

On the other hand, the time required for the complete removal of ammonia by the FVT is influenced solely by the closing time of the main valve, independent of the opening time of the bleed valve. The minimum purging time was five seconds at a closing rate of 18%/s. Figure 12b depicts the variation in purging time in relation to the closing rate of the main valve. Through the two results, it was confirmed that residual ammonia can be removed using a small amount of N_2 when optimized FVT control operation is applied.

4. Conclusions

The FVT for fuel supply and shutdown on ships showed improved performance under specific operational conditions during startup and shutdown.

Under startup conditions, the opening of the main valve influenced the time taken for the flow to increase. Up to a 50% flow increase, the maximum flow difference was observed to be 17.8 kg/h at an opening rate of 30%/s. However, the conversion rate of ammonia composition showed less than 1% difference in relation to valve opening rate. These results confirmed that flow rate improvement and ammonia conversion rate could be increased only through FVT control.

On the other hand, for the shutdown process of the engine, a model was proposed to sequentially lock the main valve and bleed valve during nitrogen purging, aiming to prevent residual ammonia within the FVT in typical port shutdown situations. Ammonia was completely removed after five seconds of nitrogen purging with a bleed valve opening rate of 10%/s and a main valve closing rate of 18%/s. At this time, the nitrogen consumption at the gas bleed valve was 0.28 kg.

In addition, variations in the nitrogen purging volume during the shutdown process were identified based on the purging pressure currently recommended for ships. The minimum supply volume was verified, with a total volume of 2.67 m^3 required at 1200 kPa. The findings indicate that purging pressure should vary depending on factors such as engine size and pipe design.

The above changes in shutdown conditions have been proposed as a means to completely remove ammonia within pipes, so as to minimize safety risks and enhance operational convenience. Through this control, the FVT itself is maintained below 50 ppm, eliminating the need for continuous monitoring and eliminating questions about leaks that occur during operation. In addition, it is possible to secure economic efficiency by applying an open design rather than using a fully ex-proof encapsulated design, which has a high initial cost.

For ships using gaseous fuels such as LPG and LNG, this analysis model is expected to be able to be utilized by applying fuel and nitrogen supply conditions and purging areas. In addition, safety can be secured through the proposed FVT control, and follow-up research on optimization methods according to fuel characteristics is expected to be necessary.

Author Contributions: Writing—Original draft, L.S.; Writing—Review and editing, L.S. and L.H.; Funding acquisition, S.Y. All authors have read and agreed to the published version of the manuscript.

Funding: This research was supported by the Korea Institute of Marine Science & Technology Promotion (KIMST) funded by the Ministry of Oceans and Fisheries, Korea (20220634).

Data Availability Statement: Data are available on request due to restrictions, e.g., privacy or ethical.

Conflicts of Interest: The authors declare no conflicts of interest.

Nomenclature

N	Nitrogen
Act	Actuator position
Act_0	Initial actuator position
$Act_{Desired}$	Desired actuator rate
C_v	Coefficient of variation
SG	Specific gravity
a	Helmholtz energy
a^0	Ideal gas Helmholtz energy
a^r	Residual Helmholtz energy
Q	Flow rate

P	Pressure
P_{purge}	Purge pressure
$P_{service\ tank}$	Service tank pressure
t	Time
Act	Actuator
o	Output
V	Volume
V_{purge}	Purge volume
V_{buffer}	Buffer tank volume
ME	Main Engine
LFSS	Low-flashpoint fuel supply system
z	Minimum number of times of purging
LHV	Lower heating value
HFO	Heavy fuel oil
R	Gas constant
M, j, i	Constant
c	Critical
FVT	Fuel valve train
GVU	Gas valve unit
GWP	Global warming potential
PID	Proportional–integral–differential controller
OP	Output
IMO	International Maritime Organization
GHG	Greenhouse gas
LNG	Liquefied natural gas
LPG	Liquefied petroleum gas
MDO	Marine diesel oil
EEDI	Energy Efficiency Design Index
EEXI	Energy Efficiency Existing Ship Index
NFPA	National Fire Protection Association

References

1. DNV GL—Maritime. *Assessment of Selected Ternative Fuels and Technologies*; DNV: Hamburg, Germany, 2018; Available online: https://sustainableworldports.org/wp-content/uploads/DNV-GL_2018_Assessment-of-selected-alternative-fuels-and-tech-report.pdf (accessed on 4 January 2022).
2. Lloyd's Register. *UMAS Techno-Economic Assessment of Zero-Carbon Fuels*; Lloyd's Register: London, UK, 2020; Available online: https://www.methanol.org/wp-content/uploads/2020/04/Techno_economic_assessment_of_zero_carbon_fuels.pdf (accessed on 15 March 2023).
3. Francesco, B.; Alain, A.; François, M. From renewable energy to ship fuel: Ammonia as an energy vector and mean for energy storage. *Comput. Aided Chem. Eng.* **2019**, *46*, 1747–1752. [CrossRef]
4. Man Energy Solution MAN B&W Two-Stroke Engine Operating on Ammonia. Available online: https://www.man-es.com/docs/default-source/marine/tools/man-b-w-two-stroke-engine-operating-on-ammonia.pdf (accessed on 14 June 2023).
5. Yara Joins Japanese Study of Ammonia-Fueled Ammonia Gas Carrier. Available online: https://www.offshore-energy.biz/yara-joins-japanese-study-of-ammonia-fueled-ammonia-gas-carrier/ (accessed on 27 October 2021).
6. Class NK, ClassNK Technical Journal "Special Feature: Zero-Emission Ships". 2022. Available online: https://www.classnk.or.jp/hp/pdf/research/rd/2022/05_e0.pdf (accessed on 12 March 2023).
7. Machaj, K.; Kupecki, J.; Malecha, Z.; Morawski, A.W.; Skrzypkiewicz, M.; Stanclik, M.; Chorowski, M. Ammonia as a potential marine fuel: A review. *Energy Strategy Rev.* **2022**, *44*, 100926. [CrossRef]
8. Øyvind Endresen, DNV GL Energy Transition Outlook 2021: Maritime Forecast to 2050. Norway. September 2019. Available online: https://sustainableworldports.org/wp-content/uploads/DNV-GL_2019_Maritime-forecast-to-2050-Energy-transition-Outlook-2019-report.pdf (accessed on 6 August 2023).
9. IMO Strategy on Reduction of GHG Emissions from Ships, RESOLUTION MEPC. 377 (80), 2023, MEPC 80-17-Add.1—Report Of The Marine Environment Protection Committee On Its Eightieth Session (Secretariat) (imo.org). Available online: https://wwwcdn.imo.org/localresources/en/OurWork/Environment/Documents/annex/MEPC%2080/Annex%2015.pdf (accessed on 28 March 2023).
10. A. S. DNV, Energy Transition Outlook 2021 Executive Summary. A Global and Regional Forecast to 2050. 2021, Denmark, pp. 1–40. Available online: https://www.connaissancedesenergies.org/sites/connaissancedesenergies.org/files/pdf-actualites/DNV_ETO_2021_Executive_summary_single_page_highres.pdf (accessed on 15 August 2023).

11. Smith, T.; Raucci, C.; Haji Hosseinloo, S.; Rojon, I.; Calleya, J.; De La Fuente, S.; Wu, P.; Palmer, K. *CO_2 Emissions from International Shipping. Possible Reduction Targets and Their Associated Pathways*; UMAS: London, UK, 2016; pp. 1–61.
12. Ryu, K.H. Combustion Characteristics and Exhaust Emissions in Spark-ignition Engine Using Gasoline-ammonia. *Trans. Korean Soc. Automot. Eng.* **2013**, *21*, 155–165. [CrossRef]
13. Jang, J.Y.; Woo, Y.M.; Yoon, H.C.; Kim, J.N.; Lee, Y.J.; Kim, J.H. Combustion Characteristics of Ammonia-Gasoline Dual-Fuel System in a One liter Engine. *J. Korean Inst. Gas* **2015**, *19*, 1–7. [CrossRef]
14. Jang, J.Y. Carbon-free Fuel for Greenhouse Gas Reduction—Ammonia(NH_3). *Auto J. J. Korean Soc. Automot. Eng.* **2020**, *42*, 52–55.
15. Niels, D.V. Safe and Effective Application of Ammonia as a Marine Fuel. Master's Thesis, Delft University of Technology, Delft, The Netherlands, 2019.
16. Seo, Y.G.; Han, S.J. Economic Evaluation of an Ammonia-Fueled Ammonia Carrier Depending on Methods of Ammonia Fuel Storage. *Energies* **2021**, *14*, 8326. [CrossRef]
17. Julia, H.; Erik, F. *On the Potential of Ammonia as Fuel for Shipping*, 1st ed.; Lighthouse Swedish Maritime Competence Centre: Göteborg, Sweden, 2020; pp. 1–28.
18. DNV. Alternative Fuel Uptake in the World Fleet in 2022. Available online: https://www.dnv.com/expert-story/maritime-impact/Collaboration-is-key-to-scale-up-fuel-availability-in-time.html (accessed on 28 March 2024).
19. Laval, A.; Hafnia, H.T.; Vestas, S.G. *Ammonfuel—An Industrial View of Ammonia as a Marine Fuel*, ALFA LAVAL, Sweden, 2020; pp. 1–59. Available online: https://www.topsoe.com/hubfs/DOWNLOADS/DOWNLOADS%20-%20White%20papers/Ammonfuel%20Report%20Version%2009.9%20August%203_update.pdf (accessed on 23 April 2023).
20. Laursen, R.; Barcarolo, D.; Patel, H.; Dowling, M.; Penfold, M.; Faber, J.; Király, J.; van der Veen, R.; Pang, E.; van Grinsven, A. EMSA, Potential of Ammonia as Fuel in Shipping. 2022. Available online: https://www.emsa.europa.eu/newsroom/latest-news/item/4833-potential-of-ammonia-as-fuel-in-shipping.html (accessed on 15 May 2023).
21. Yude, S.; Kang, H.K.; Lee, Y.H.; Grzegorz, K.; Paolo, G.; Li, Z.X. A preliminary risk assessment on development the fuel gas supply system of a small LNG fueled fishing ship. *Ocean. Eng.* **2022**, *258*, 111645. [CrossRef]
22. Kang, I.P.; Kim, K.C. Development of a FVT (Gas Valve Train) Control System for LNG Fueled Vessels. *J. Power Syst. Eng.* **2017**, *21*, 70–76.
23. Lim, S.T.; Lee, H.S.; Moon, J.H.; Seo, Y.K. Analysis of Fuel Consumption for Application of Ammonia Propulsion Model in Ammonia Transport Ships. *J. Power Syst. Eng.* **2022**, *26*, 83–91. [CrossRef]
24. KÜHME, KÜHME Solutions for Gas Fueled Ships, Germany. 2020. Available online: https://kuehme.de/wp-content/uploads/2020/04/Kuehme-Armaturen-GmbH-Bochum-Gas-Valve-Unit-Portfolio.pdf (accessed on 4 October 2023).
25. Rother, S.; Watter, H. Experiences with gas engines during practical ship operations—Impact of load fluctuations during generator operations on the ship's power grid. *Sci. J. Zesz. Nauk. Marit. Univ. Szczec.* **2018**, *55*, 44–50. [CrossRef]
26. Lee, M.H.; Shao, Y.D.; Kim, Y.T.; Kang, H.K. Performance characteristics under various load conditions of coastal ship with LNG-powered system. *J. Korean Soc. Mar. Eng.* **2017**, *41*, 424–430. [CrossRef]
27. Liptak, B.G. *Instrument Engineers Handbook, Process Measurement and Analysis*; Butterworth-Heinemann: Oxford, UK, 1995.
28. Control Valve Sizing. In *Control Valve Handbook (PDF)*, 5th ed.; Emerson Electric: Ferguson, MO, USA, 2019.
29. Dynamic Modeling. In *HYSYS 2004.2 (PDF)*; Aspentech: Bedford, MA, USA, 2005; pp. 1–69.
30. MAN B&W. G60ME-C9.2-GI-TII. In *Project Guide Electronically Controlled Dual Fuel Two-Stroke Engines (PDF)*; MAN Diesel & Turbo: Copenhagen, Denmark, 2014.
31. Baehr, H.D.; Tillner, R.R. *Thermodynamic Properties of Environmentally Acceptable Refrigerants*; Equations of State and Tables for Ammonia, R22, R134a, R152a, and R123; Springer: Berlin/Heidelberg, Germany, 1994.
32. Span, R.; Lemmon, E.W.; Jacobsen, R.T.; Wagner, W.; Yokozeki, A.A. Reference Quality Thermodynamic Property Formulation for Nitrogen. *J. Phys. Chem. Ref. Data* **2002**, *29*, 1361–1433. [CrossRef]
33. Wärtsilä Marine Solutions, Wärtsilä 50DF PRODUCT GUIDE. 2019. Available online: https://cdn.wartsila.com/docs/default-source/product-files/engines/df-engine/product-guide-o-e-w50df.pdf?sfvrsn=9 (accessed on 17 June 2022).
34. HYUNDAI ENGINE & MACHINERY, PROJECT GUIDE HiMSEN H54DFV FOR STATIONARY. 2022. Available online: https://www.hyundai-engine.com/ko/Customer/TechData?page=9&category=all (accessed on 26 January 2024).
35. Win, G.D. 2-Stroke Dual-Fuel Safety Concept. 2021. Available online: https://www.wingd.com/en/documents/concept-guidances/dg9727-df-safety-concept/ (accessed on 20 December 2023).
36. Ozawa, Y. Low NOx combustion technology for LNG combined cycle power plant. *J.-Jpn. Inst. Energy* **2001**, *80*, 1020–1031.
37. Chun, J.M.; Kang, H.K.; Kim, Y.T.; Jung, M.H.; Cho, K.H. Case study on operating characteristics of gas fueled ship under the conditions of load variation. *J. Korean Soc. Mar. Eng.* **2016**, *40*, 447–452. [CrossRef]
38. Centers for Disease Control and Prevention (CDC), Toxicological Profile for Ammonia. 2004. Available online: https://www.atsdr.cdc.gov/ToxProfiles/tp126-c2.pdf (accessed on 21 March 2023).